CHARACTERIZATION OF OXIDE FORMED ON SILICON BY EXPOSURE TO ATOMIC OXYGEN IN SPACE

LOUISE C. SENGUPTA
CERAMICS RESEARCH BRANCH

JUDITH S. BRODKIN, WOLFGANG FRANZEN, and PAUL L. SAGALYN
METALS RESEARCH BRANCH

DTIC
ELECTE
MAY 1 1 1992
S
D
D

February 1992

92-12390

The findings in this report are not to be construed as an official
Department of the Army position, unless so designated by other
authorized documents.

Mention of any trade names or manufacturers in this report
shall not be construed as advertising nor as an official
indorsement or approval of such products or companies by
the United States Government.

REPORT DOCUMENTATION PAGE		READ INSTRUCTIONS BEFORE COMPLETING FORM
1. REPORT NUMBER MTL TR 92-1	2. GOVT ACCESSION NO.	3. RECIPIENT'S CATALOG NUMBER
4. TITLE (and Subtitle) CHARACTERIZATION OF OXIDE FORMED ON SILICON BY EXPOSURE TO ATOMIC OXYGEN IN SPACE		5. TYPE OF REPORT & PERIOD COVERED Final Report
		6. PERFORMING ORG. REPORT NUMBER
7. AUTHOR(s) Louise C. Sengupta, Judith S. Brodkin, Wolfgang Franzen, and Paul L. Sagalyn		8. CONTRACT OR GRANT NUMBER(s)
9. PERFORMING ORGANIZATION NAME AND ADDRESS U.S. Army Materials Technology Laboratory Watertown, Massachusetts 02172-0001 SLCMT-EMC		10. PROGRAM ELEMENT, PROJECT, TASK AREA & WORK UNIT NUMBERS D/A Project: A1205.AH84
11. CONTROLLING OFFICE NAME AND ADDRESS U.S. Army Laboratory Command 2800 Powder Mill Road Adelphi, Maryland 20783-1145		12. REPORT DATE February 1992
		13. NUMBER OF PAGES 18
14. MONITORING AGENCY NAME & ADDRESS (if different from Controlling Office)		15. SECURITY CLASS. (of this report) Unclassified
		15a. DECLASSIFICATION/DOWNGRADING SCHEDULE

16. DISTRIBUTION STATEMENT (of this Report)

Approved for public release; distribution unlimited.

17. DISTRIBUTION STATEMENT (of the abstract entered in Block 20, if different from Report)

18. SUPPLEMENTARY NOTES

19. KEY WORDS (Continue on reverse side if necessary and identify by block number)

Variable angle spectroscopic ellipsometry (VASE)	Silicon	Atomic oxygen
X-ray photoelectron spectroscopy (XPS)	Oxide films	Fourier transform infrared reflectance
Rutherford backscattering spectroscopy (RBS)	Long duration exposure facility (LDEF)	
Spectroscopy		
Ellipsometry	Space environments	

20. ABSTRACT (Continue on reverse side if necessary and identify by block number)

(SEE REVERSE SIDE)

Block No. 20

ABSTRACT

The oxide formed on silicon by exposure to space on the long duration exposure facility (LDEF) has been examined using variable angle spectroscopic ellipsometry (VASE), Fourier transform infrared spectroscopy (FTIR), and X-ray photoelectron spectroscopy (XPS). The position of the silicon specimen on the satellite resulted in the formation of an oxide whose thickness varied with distance along the sample surface. Each transverse section of the surface was studied separately and compared to a region on the sample shielded from the oxygen flux in space by an aluminum bar. Film thickness and composition of the oxide were determined by a least square fit of the VASE data to a model surface using an effective medium approximation. The results revealed a nonporous oxide film with a thickness that increased from 350 Å to 1200 Å almost linearly along the sample. Furthermore, all of the experiments revealed an oxygen deficiency that increases with film thickness. Several other techniques were also performed on the sample to confirm these results. These results can be used to identify some of the oxide deposition parameters which occurred in the environment of the LDEF.

CONTENTS

INTRODUCTION

It is well known that films of silicon dioxide on silicon are important in the fabrication of many electronic devices. In fact, much of the current electronic industry is based upon the processing of silicon and silicon dioxide. Silicon is still the most widely used and most reproducible semiconducting material presently available. Therefore, the interest in producing defect-free silicon dioxide at low temperatures is obviously great. Silicon dioxide films may also serve as effective diffusion barriers in the protection of silvered space-reflectors on the low earth orbit (LEO) space station.[1] The LEO would be likely to have significant exposure to atomic oxygen in the ground state with impact energy of approximately 5 eV.[2,3] An amorphous coating is required to prevent oxygen diffusion because grain boundaries in the crystalline oxide would provide short circuit diffusion paths; therefore, low temperature growth of SiO_2 is needed.

Earlier workers have attempted this low temperature oxide deposition[4,5] and others have simulated space exposure by exposing silicon to oxygen in a plasma asher.[6,7] In our studies, the formation of silicon dioxide on silicon by exposure to atomic oxygen on the long doration exposure facility (LDEF) has been analyzed for the first time. This not only allows the study of diffusion of atomic oxygen but also to analyze the effect of actual oxidation conditions in space.

The primary technique used to characterize the films was variable angle spectroscopic ellipsometry (VASE). In this system, the elliptically-polarized light produced by reflecting plane-polarized light from the surface under study is modulated by a rotating analyzer. Both the wavelength of the monochromatic incident light and the angle of incidence can be varied. The state of polarization of the reflected beam, characterized by the ellipsometric parameters ψ and Δ can be determined by Fourier analyzing the time variation of the modulated light. The Fourier analysis allows measurement of the real part, $\tan \psi \cos \Delta$, and the imaginary part, $\tan \psi \sin \Delta$, of the complex reflectivity ratio r_p/r_s, where p denotes polarization parallel to the plane of incidence and s denotes polarization perpendicular to the plan of incidence.

$$\frac{r_p}{r_s} = e^{i\Delta} \tan \psi \tag{1}$$

The index of refraction, n, and the extinction coefficient, k, can then be calculated from ψ and Δ. For thin films, the values of n and k so determined are not related to the values obtained for any one substance but are dependent upon the penetration depth of the light. SiO_2 is an insulator and has essentially zero absorption in the visible region.

EXPERIMENTAL

The silicon sample was mounted on the earth end of the LDEF satellite on tray G12 (oxygen fluence = 5 x 10^{19}/cm^2, as shown in Figure 1. The sample dimensions were 0.3 x 5 x 5 cm^3. An aluminum bar was strapped across the center of the sample, shielding the covered portion from direct exposure to space. The oxide formed on the sample

1. DE, B. N., HRUSKA, J., PETERKIN, J., ZHAO, Y., and WOOLLAM, J. A. Mat. Res. Soc. Symp. Proc., v. 163, 1990, p. 965.
2. GULINO, D. A., EGGER, R. A., and BANHOLZER, W. F. J. Vac. Sci. Technol. A, v. 5, no. 4, 1987, p. 2737.
3. BANKS, B. A., MIRTICH, M. R., RUTLEDGE, S. K., and NAHRA, H. K. Proc. of the 18th IEEE Photovoltaic Specialists Conf., IEEE, New York, NY, 1985, p. 381-386.
4. HO, V. Q., and SUGANO, T. IEEE Trans. Elec. Dev., Ed-27, 1980, p. 1436.
5. LAWLESS, K. R. Rep. Prog. Phys., v. 37, 1974, p. 231.
6. DE, B. N., MEMARZADEH, K., JULIANTO, A., MEYERS, G. G., and WOOLLAM, J. A. AIAA Journal, v. 28, 1990, p. 1065.

by exposure to the space environment varied along the sample surface, causing a gradation in interference colors corresponding to various oxide thicknesses. Each colored region was studied individually, as shown in Figure 2 (region 1B = gray, region 2B = brown, region 3B = violet, region 4B = blue, region 7 = shielded (under aluminum bar), region 1T = blue/violet, region 2T = brown/violet, and region 3T = brown/gray). All of the measurements were performed seperately on each of these regions of the sample and each one of the experiments involved a different spot size. Therefore, the same spot within each sample section may not have been examined.
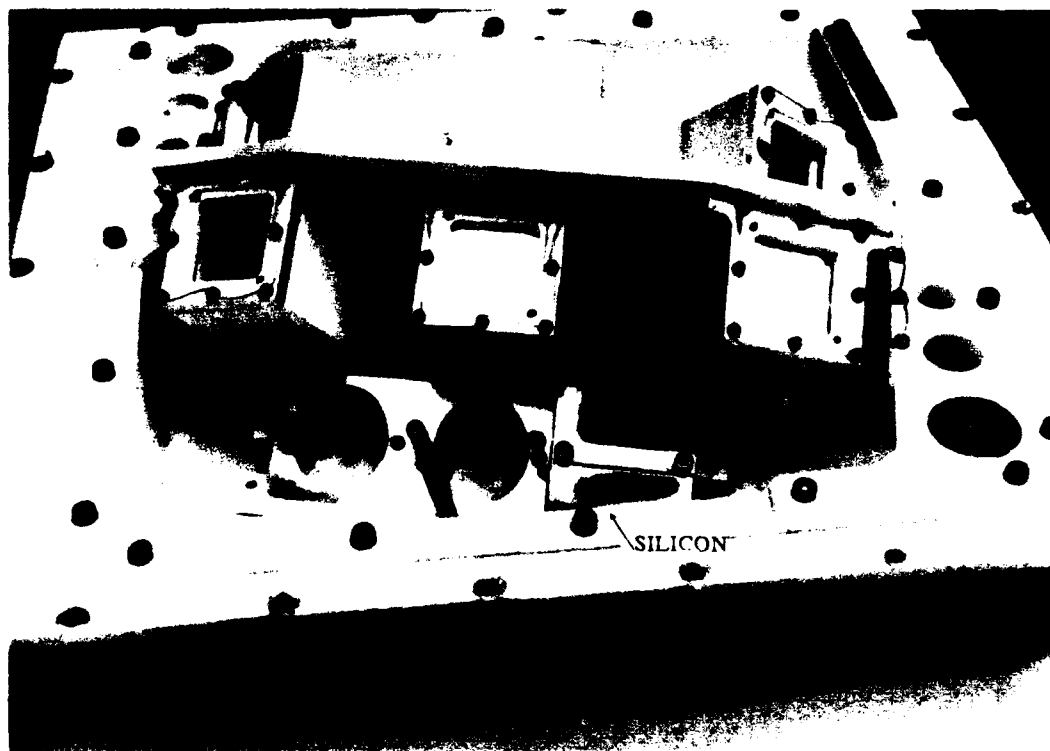

Figure 1. Photograph of silicon sample on LDEF satellite
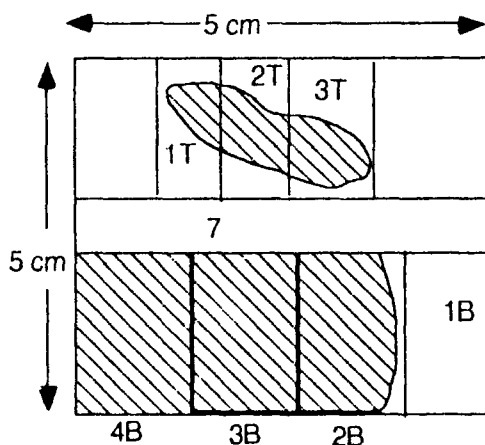(tray G12 - earth end, oxygen flux = $5 \times 10^{19}/cm^2$).

Figure 2. Schematic of examined portions of LDEF silicon sample (oxide color: 1T = blue/violet, 2T = brown/violet, 3T = brown/gray, 1B = gray, 2B = brown, 3B = violet, 4B = blue, and 7 = shielded from space by aluminum strap).

A schematic of the ellipsometer designed by J. A. Woollam is shown in Figure 3. The ellipsometer uses a rotating analyzer. At each wavelength after 150 revolutions of the analyzer, a data acquisition program subtracts a reading obtained with the shutter closed from a reading taken with the shutter open in order to eliminate any effect of background radiation. During a measurement the wavelength was scanned from 4000 Å to 8000 Å in steps of 100 Å. Two or three angles of incidence were examined at each spot. The data was fit to a model (see Figure 4) consisting of a silicon substrate covered by a nonporous SiO_2-SiO film. The analysis software uses a Marquardt algorithm and a Bruggeman Effective Medium approximation[8] and relies on published data for the substrate and film constituents. The fitting parameters were the film thickness and the SiO fraction. In some cases the angle of incidence was varied slightly to obtain more accurate agreement.
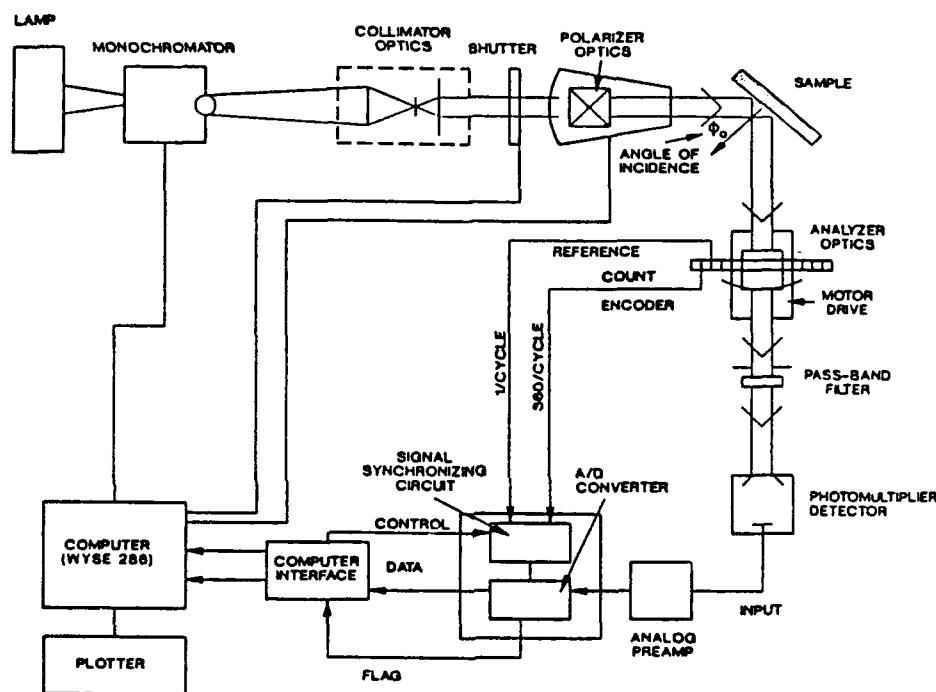

Figure 3. Block diagram of VASE system designed and built by the Woollam Company, Lincoln, NE.
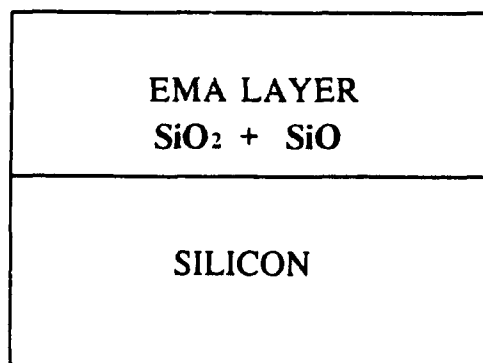

Figure 4. Model used to fit VASE results: silicon substrate with an oxide film consisting of an EMA layer of (1-x)% SiO_2 and x% SiO.

8. WOOLLAM, J. A., SYNDER, P. O., and ROST, M. C. Thin Solid Films, v. 166, 1988, p. 317.

The Fourier transform infrared spectroscopy (FTIR) spectra were taken with a Perkin-Elmer 1600 series spectrometer at an angle of incidence of 30° in the range from 400 cm^{-1} to 4000 cm^{-1} at a resolution of 4 cm^{-1} using nitrogen as a purge gas in the sample compartment. The spectral reflectance was measured with 128 scans of each spot in every one of the sample areas listed above.

The X-ray photoelectron spectroscopy (XPS) experiment using a Perkin-Elmer 548 system was carried out with characteristic kα radiation from a Mg target in a vacuum of approximately 10^{-8} Torr. When scanning the entire electron energy range, the sensitivity was 30 K, the time constant was 0.1 seconds, and the pass energy was 100 eV. These conditions were varied (sensitivity = 1 to 10 K, time constant = 0.1 to 1.0 sec, and pass energy = 25 eV) when the elemental peak positions were accurately determined. The C_{1s} peak was used as a calibration peak for the determination of the peak positions of the other elements.

Rutherford Backscattering Spectroscopy (RBS) was carried out by bombarding the sample with a beam of 2 MeV He^{+} ions at an angle of incidence of either 0° or 60° and a backscattering angle of 170°.

RESULTS AND DISCUSSION

Representative VASE spectra and their fits to the model described above are shown in Figures 5 through 7 from 4000 Å to 8000 Å for some of the examined regions of the sample. The optical constants of region 1B and of pure Si are compared in Figure 5 and Figure 6; the same data are compared with data generated from the model of Figure 4. For regions of the sample covered with thick oxide films and exhibiting quarter wavelength interference patterns, the measured values of tan ψ and cos Δ are plotted in Figure 7 for region 3B and in Figure 8 for region 1T. A summary of the VASE data is given in Table 1. The uncertainty associated with the percentage of SiO present in the film is less than 0.1%.

Table 1. OXIDE THICKNESS AND COMPOSITION (VASE RESULTS) AND
% POROSITY OF THE LDEF SILICON SPECIMEN

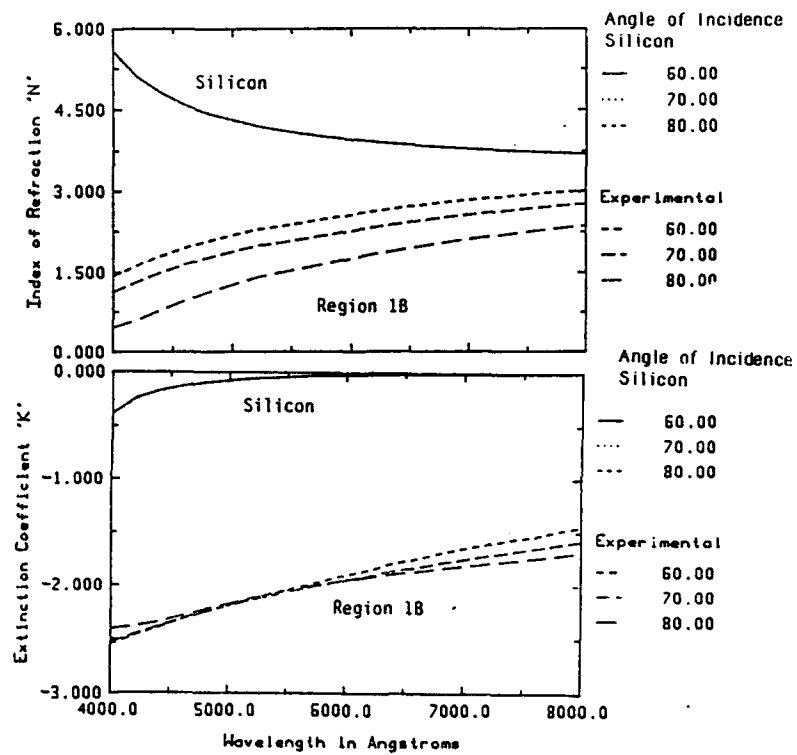| Region	Oxide Color	Oxide Thickness (Å)	SiO (%)	Porosity (%)
1T	Blue/Violet	996.8 ± 1.2	14.9	not meas.
2T	Brown/Blue	716.9 ± 3.4	13.3	not meas.
1B	Gray	386.1 ± 5.5	0	9.43
2B	Brown	650.5 ± 8.4	0	0.33
3B	Violet	993.3 ± 1.8	22.9	1.52
4B	Blue	1221 ± 2.0	18.3	0.87
7	Shielded	77.6 ± 1.8	100	1.58

Figure 5. Optical constants of region 1B compared to those of pure silicon.
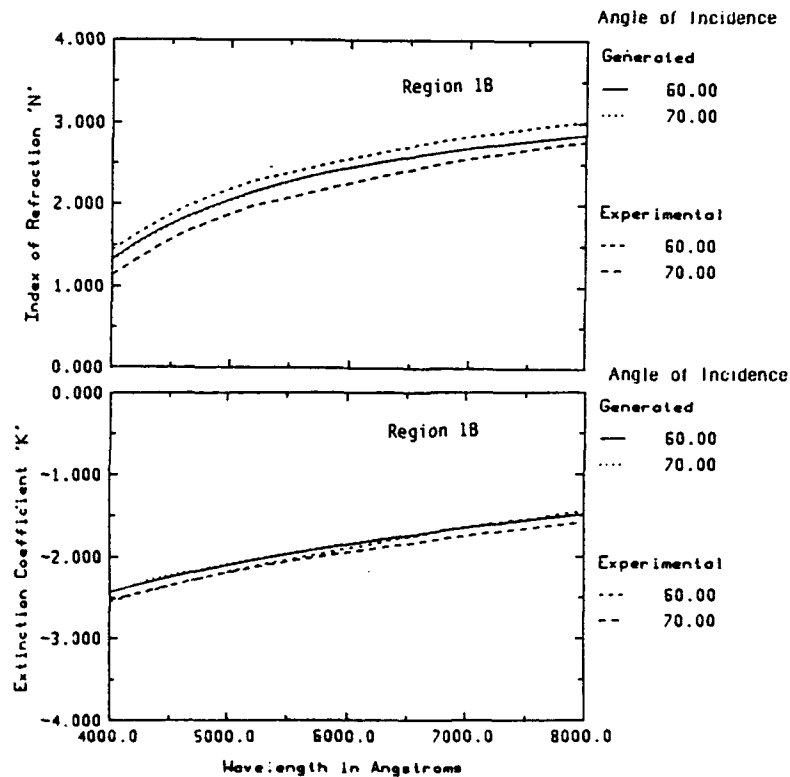

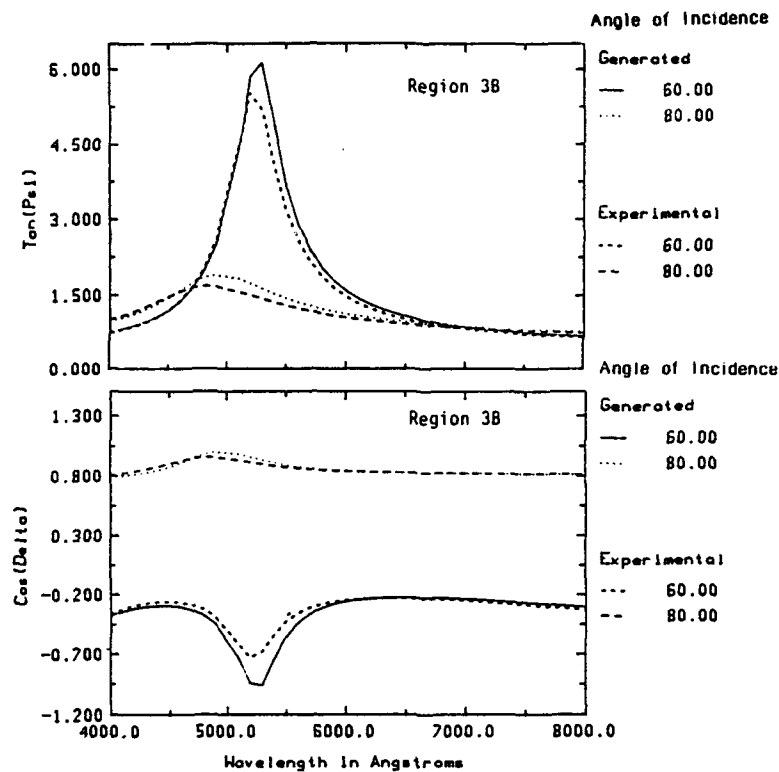Figure 6. Optical constants of region 1B compared to those generated from the model.

Figure 7. Tan ψ and cos Δ for the experimental data and data generated from the model for region 3B of LDEF silicon sample.
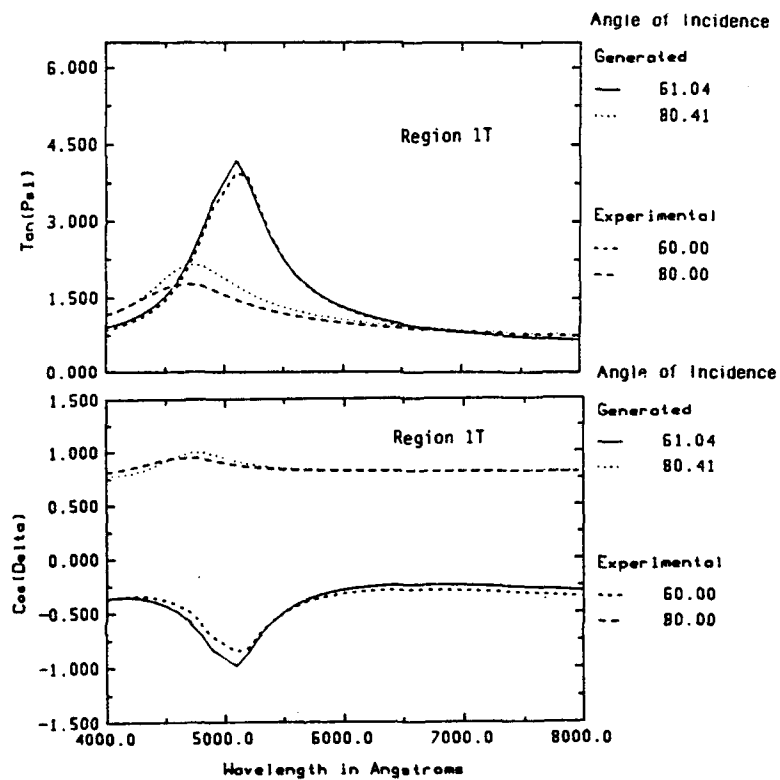

Figure 8. Tan ψ and cos Δ for the experimental data and data generated from the model for region 1T of LDEF silicon sample.

6

As shown in Figure 9, the VASE data suggest that the oxide thickness increases almost linearly along the sample surface. Since the sample was mounted on an inclined tray on the earth end of the satellite, areas of the sample closer to the top of the tray were exposed to a greater flux of atomic oxygen than areas at the other end of the tray. If most of the oxygen had been scattered from the detector to the right of the sample before striking the sample surface (see Figure 1) the oxide film next to the detector (region 4B) would be much thicker than the film at the other end (region 1B), even thicker than it is. Therefore, it appears that oxygen was deposited directly onto the sample surface.
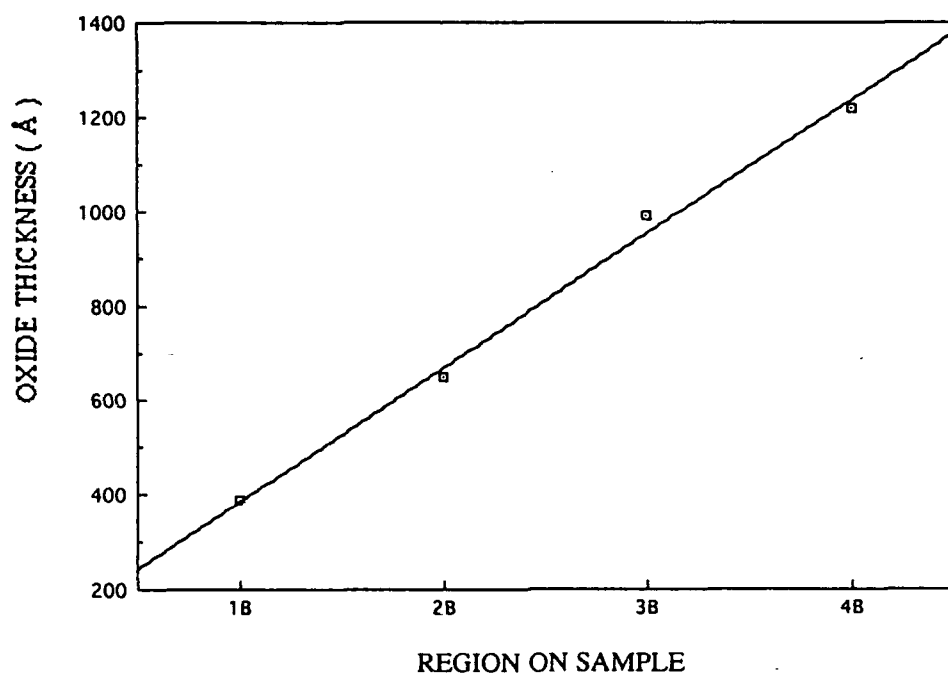

Figure 9. Oxide thickness obtained from VASE results versus position on LDEF silicon sample

Our results also indicate that unlike other low temperature depositions the oxide thus formed was not porous; an observation confirmed by porosity measurements made with a Buehler metallograph. In this technique the average percentage of voids is determined from the contrast in the field of view of a microscope at magnification of 500X to 1000X with the aid of a computer program. Readings were taken at at least 10 locations on each of the examined regions. As shown in Table 1, these measurements indicate a porosity of less than 10% for all regions. The fact that the oxide was found to be nonporous may be due to the fact that the deposition rate of the process is extremely slow relative to other techniques. However, a copper sample mounted immediately adjacent to the silicon specimen had a very porous oxide layer which was also much thicker than that formed on the section of the silicon closest to the copper sample.[9] The only other sample that did not show porous oxide formation was an aluminum specimen mounted on the trailing edge of the satellite.[9] These variations in the porosity of the oxide films formed on different LDEF samples are not presently understood. The lack of porosity of the oxide film on the silicon sample may be affected by the presence of carbon throughout the film and will be discussed later.

9. FRANZEN, W., BRODKIN, J. S., SENGUPTA, L. C., and SAGALYN, P. L. Proceedings of the First LDEF Post-Retrieval Symposium (in Press).

Furthermore, the VASE results summarized in Table 1 indicate that the SiO/SiO_2 ratio increases from 0 to 0.2 with increasing film thickness suggesting that although the oxidation took place slowly and at a low temperature, a greater amount of oxygen incident on the sample surface corresponds to a larger oxygen deficiency. For the film formed under the shielded section of the sample (region 7), the model that made the best fit consisted of 100% SiO. This may be due to the fact that oxygen is often found in pure silicon as an interstitial. Therefore, the SiO formation requires less energy than the formation of SiO_2. This may be why it was possible to form this oxide under a barrier (region 7).

In order to confirm the accuracy of the VASE results several other characterization techniques were employed. FTIR reflectance spectra are shown in Figure 10 and are summarized in Table 2. As for other oxidation processes including thermal oxidation of silicon,[10] the SiO stretching mode at 1065 cm^{-1} shifts upward in frequency with increasing film thickness, as shown in Figure 11. This effect has been attributed to an increase in bond strain and/or oxygen deficiency with distance away from the film/substrate interface.[10] It should be noted that the shift in frequency is nonlinear for film thicknesses greater than 150 Å, as has also been reported for thermal oxides,[10] a result of the fact that as the film thickness increases beyond a certain critical value the structure of the film becomes less constrained by the substrate, allowing the material to relax and the peak shift to decrease.

Table 2. PEAK POSITION AND FWHM OF THE SiO STRETCHING MODE FROM THE FTIR RESULTS OF THE LDEF SILICON SAMPLE

Region	Peak Position (cm^{-1})	FWHM (cm^{-1})
1T	1066	91.7
2T	1063	85.2
1B	1059	63.7
2B	1061	72.7
3B	1065	82.8
4B	1069	72.7
7	1044	63.7

However, for the space-formed oxide an increase in bond strain may not be the only factor contributing to a peak shift since the full width at half-maximum (FWHM) increased with thickness (broadening associated with off-stoichiometry oxides is usually 20% to 30%).[10] This may indicate that the material contains some oxygen deficiency, especially since the shift in frequency is accompanied by an increase in mode broadening with increase in oxide thickness.

The FTIR results do not show any mode at 935 cm^{-1} (SiO stretching mode of SiOH) usually indicative of the effect of humidity on porous oxide. Therefore, this result may also verify the nonporous nature of the oxide. The values for the peak position and width of the SiO mode agree well with those found for thermal oxides.[10-12]

10. BOYD, I. W., and WILSON, J. I. B. J. Appl. Phys., v. 53, 1982, p. 4166.
11. PLISKNEN, W. A. J. Vac. Sci. Technol., v. 14, 1977, p. 1064.
12. LUCOVSKY, G., MANITINI, M. J., SRIVASTAVA, J. K., and IRENE, E. A. J. Vac. Sci. Technol., v. B5, 1987, p. 530.
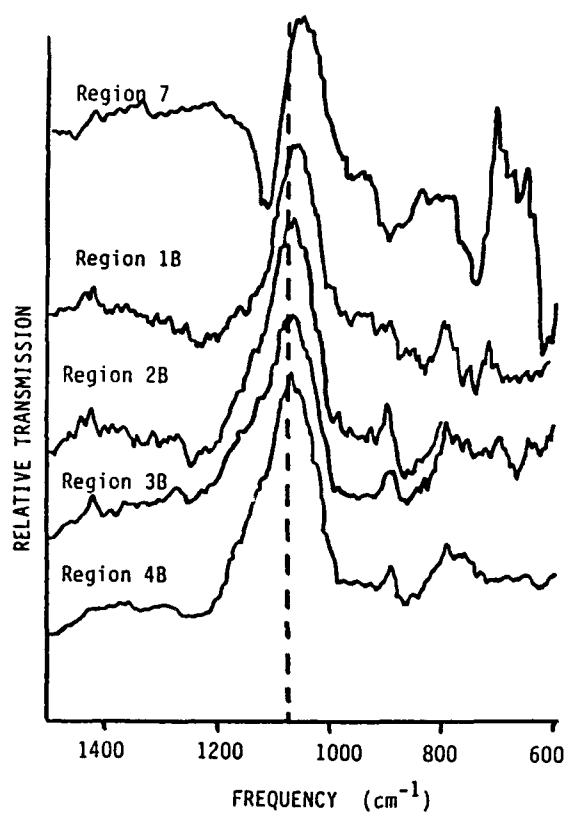
Figure 10. FTIR reflectance spectra showing Si-O stretching mode for regions 1B through 4B and region 7 of LDEF silicon sample.
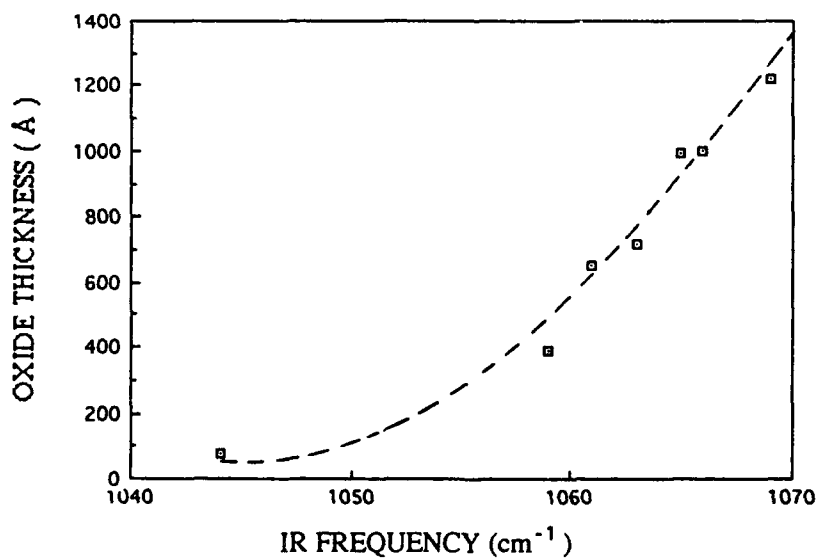

Figure 11. Peak position of Si-O stretching mode versus oxide thickness for various regions on silicon sample.

In order to confirm the composition of the oxide, XPS was performed on the specimen for the regions specified in Figure 2. The spectra of regions 1T, 1B, 6B, and from the back of the specimen are shown in Figure 12. It is evident that carbon, oxygen, and silicon are present on the surface in varying proportions. The positions of the C_{1s}, O_{1s}, and Si_{2p} peaks and the relative percentages of carbon, silicon, and oxygen present in the surfaces are listed in Table 3, together with the shift ΔC_{1s} of the C_{1s} peak from its usual value of 284.6 eV.

Table 3. XPS RESULTS FOR THE LDEF SILICON SPECIMEN

Region	Si_{2p} Peak Position (eV)	Si%	O_{1s} Peak Position (eV)	O%	C_{1s} Peak Position (eV)	C%	ΔC_{1s} (From 284.6) (eV)
1T	103	30	532.4	46	286.8	24	2.2
2T	103.2	30	532.4	49	287.0	21	2.4
3T	103.5	29	532.4	49	286.6	22	2.0
1B	103.4	28	532.5	38	285.5	34	0.9
2B	103.4	31	532.4	50	286.4	19	1.8
3B	103.2	30	532.6	43	286.8	26	2.2
4B	103.1	30	532.8	50	287.2	20	2.6
Back	98.8 102.9	28	531.8	19	285.0	53	0.4
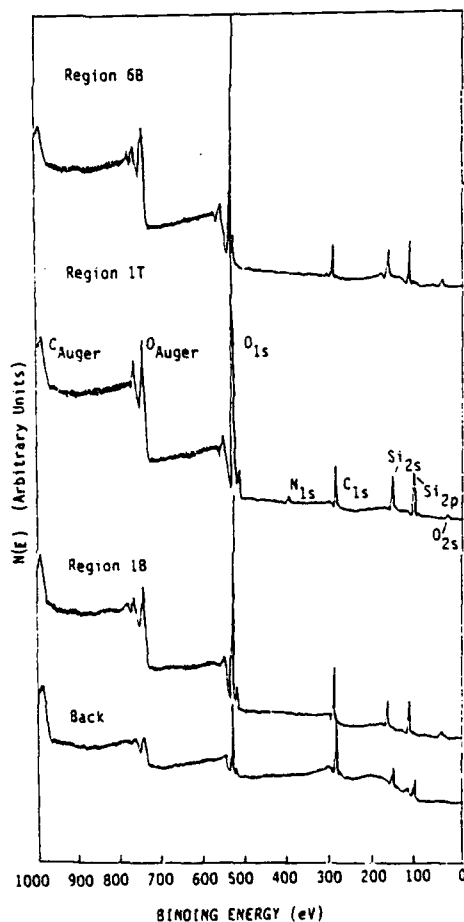
Figure 12. XPS spectra of regions 1T, 1B, 4B, and back of the LDEF silicon sample.

It is evident that a relatively large amount of carbon is present on the sample surface. This is not an unusual observation and can be attributed to contamination at any stage of the specimen's lifetime. Figure 13 shows the positions of the C_{1s} and Si_{2p} peaks as functions of oxide thickness. It is evident that the C_{1s} peak shifts to increasing energy with increase in film thickness. This carbon peak is commonly used as the calibration peak and the amount that the peak has shifted from 284.6 eV is subtracted from the peak position of the other elements. The shift is expected and is caused by a buildup of surface charge with increase in film thickness. It is also observed that the ratio of oxygen to carbon, except for the back of the specimen, ranges from 1.1 to 2.46 but does not vary systematically with oxide thickness. There is a peculiarity associated with the presence of carbon deduced from the RBS data that will be discussed later in the connection with the analysis of that data.
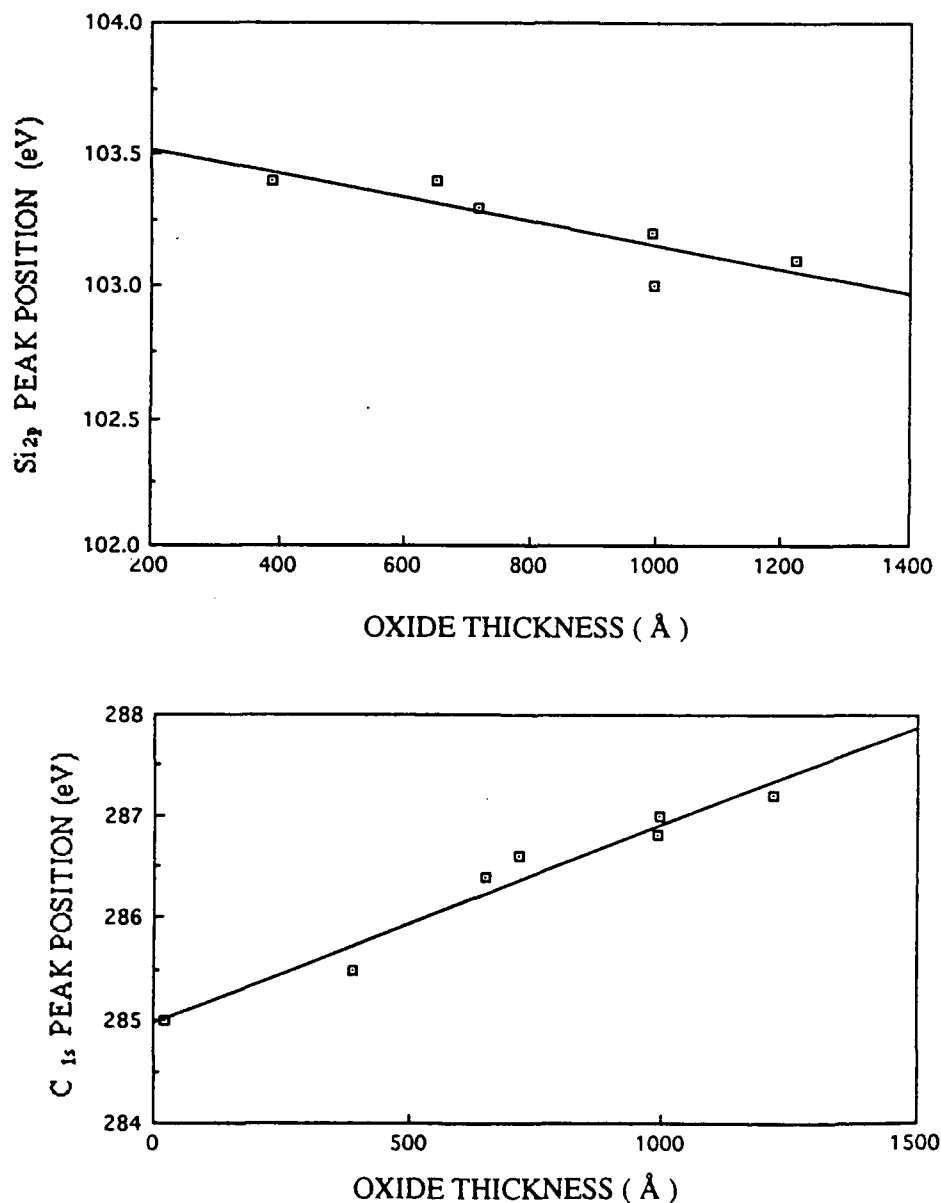
Figure 13. Si_{2p} and C_{1s} peak positions (eV) versus oxide thickness.
Uncertainty associated with peak position = ± 0.1 eV.

11

Figure 13 also shows that the Si_{2p} peak shifts to lower energies with an increase in film thickness. Since this peak is located at 99.15 eV for pure Si and at 103.4 eV for stoichiometrically correct SiO_2, the shift from 103.5 eV to lower energies indicates that the oxide film is becoming more oxygen deficient with increase in oxide thickness. The XPS data taken on the back portion of the sample shows the Si_{2p} peak at two positions; namely, at approximately 99 eV and 103.4 eV, indicating the presence of the very thin native oxide layer ($\sim$20 Å) associated with pure silicon. The ratio of oxygen to silicon, except for the unexposed region (back of sample), ranges from 1.34 to 1.65 indicating that the oxide film is oxygen deficient.

The position of the O_{1s} peak remains essentially constant at the location that corresponds to the formation of SiO_2 (532.6 eV) indicating that most of the oxygen on the surface is combined with silicon to form the oxide layer. The data from the back portion of the sample is an exception to this observation in that the oxygen peak is at a lower energy indicating the presence of a thin layer of oxide containing uncombined oxygen. Some areas of the silicon surface appear to contain a small amount of nitrogen.

The results of the analysis of RBS spectra for regions 1T, 3T, and 7, as well as for regions 1B, 2B, 3B, and 4B of the specimen, are shown in Figures 14 and 15, respectively. Estimated film thicknesses obtained from the RBS data agree within an uncertainty of $\pm$ 80 Å with those calculated from the VASE spectra. The data suggest that for most of the exposed regions of the sample a large fraction of carbon is present that increases as the film/substrate interface is approached. As the amount of carbon increases, the amount of oxygen seems to decrease.

These results on the presence of carbon in the film agree with the XPS observations. However, the large amount of carbon increasing with distance into the film was indeed unexpected. This carbon profile makes it difficult to determine the oxygen stoichiometry in the film from the RBS data alone.

This phenomenon may be caused by several factors. One explanation may be that the oxide formed by this low-temperature deposition was actually porous and the film has been infiltrated with carbon and has formed a nonporous carbonated film. However, the source of this contamination is unclear at the present time.

Another possibility is that the film was formed by impact of carbon-rich projectiles. Figure 16 shows a micrograph of the specimen's surface taken at 500X (see region 1B). It is clear that craters of about 20 microns wide by 100 microns long are present. The presence of impact craters formed by carbon-rich impactors has been reported previously for an Al sample mounted on LDEF tray A11EOOF.[13] The impactor residue in the craters contained 54% to 72% carbon inside the craters and about 40% 1 mm away from the craters. This type of carbon contamination could account for the carbon distribution revealed by the analysis of the RBS results which suggest that each impact crater removed part of the oxide as it struck the film leaving behind a carbon-rich residue. However, the amount of carbon present in the film is rather high to be caused exclusively by these impactors and the resultant distribution may be caused by a combination of both of the factors described above.

13. RADICATI DI BROZOLO, F., FLEMMING, R. H., HARRIS, D. W., BROWNLEE, D., and REILLY, T. W. M&D SIG Investigation Report, First LDEF Post-Retrieval Symposium Abstracts, p. 40.
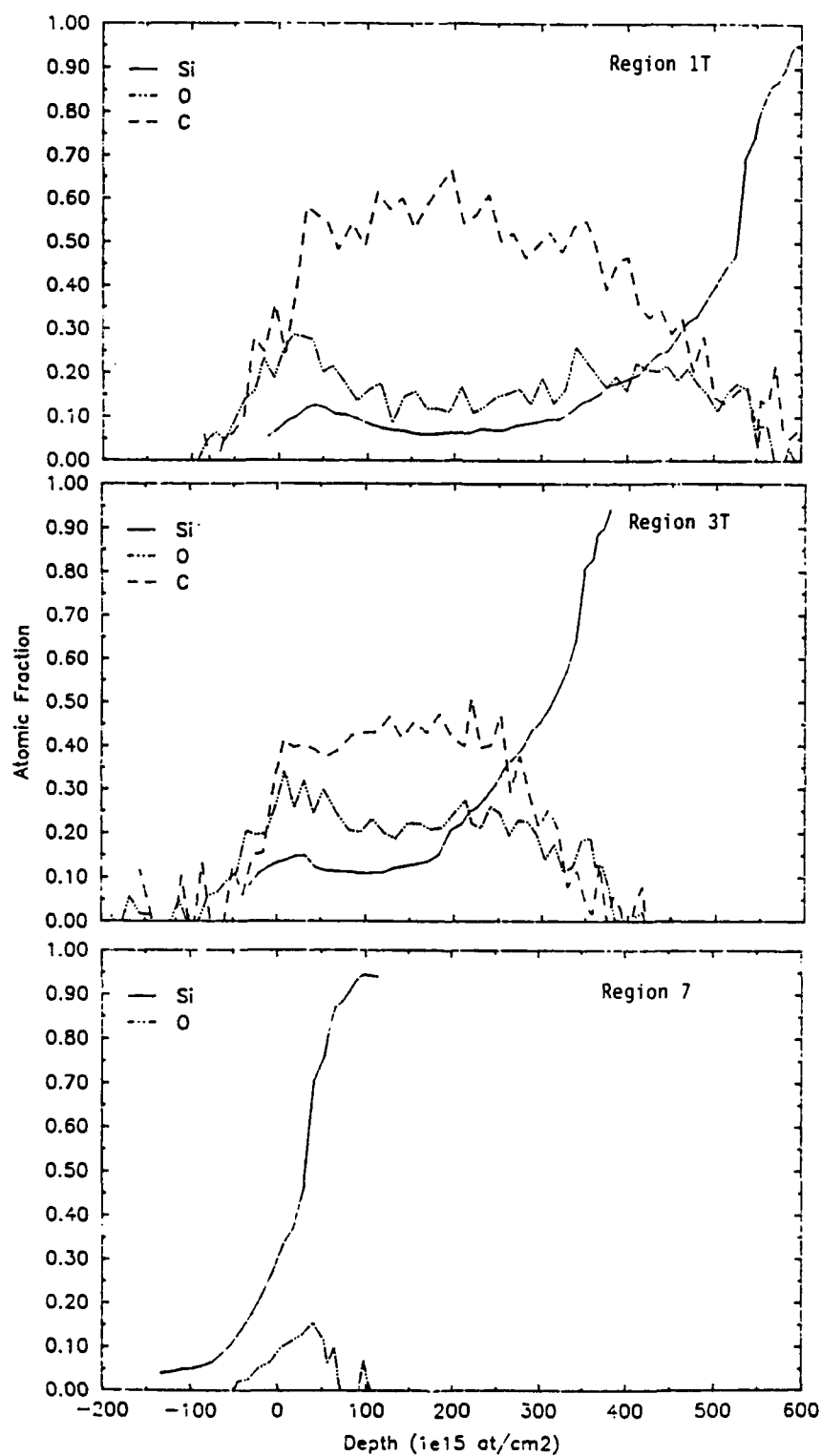
Figure 14. Atomic fractions deduced from RBS spectra
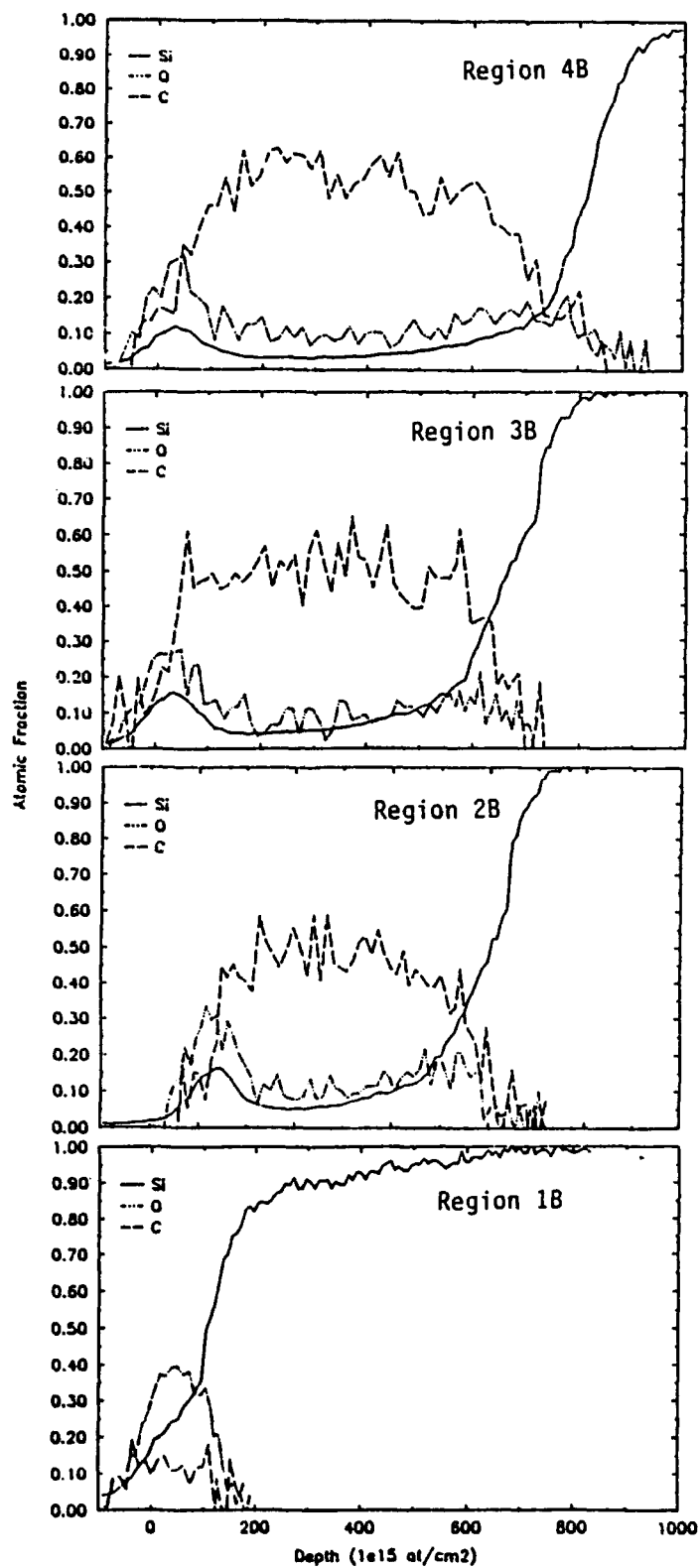of regions 1T, 3T, and 7 of the LDEF Si sample.

Figure 15. Atomic fractions deduced from RBS spectra of
regions 1B, 2B, 3B, and 4B of the LDEF Si sample.

Figure 16. Micrograph (500X) of LDEF silicon surface (region 1B).

CONCLUSIONS

The results from the VASE analysis of the oxide film formed on the LDEF silicon specimen revealed an oxide thickness that varied linearly along the sample surface. As confirmed by FTIR results, the film is not porous but is oxygen deficient. Compositional analysis by XPS and RBS confirmed the finding of oxygen deficiency and also showed that the surface and interior of the film contained substantial amounts of carbon. The carbon contamination may have been caused by several factors and, as indicated in this report, can partially originate from carbon-rich imp\ctors present in the space environment.

15

DISTRIBUTION LIST

No. of Copies	To
1	Office of the Under Secretary of Defense for Research and Engineering, The Pentagon, Washington, DC 20301

Commander, U.S. Army Laboratory Command, 2800 Powder Mill Road, Adelphi,
MD 20783-1145
1 ATTN: AMSLC-IM-TL
1   AMSLC-CT

Commander, Defense Technical Information Center, Cameron Station, Building 5,
5010 Duke Street, Alexandria, VA 22304-6145
2 ATTN: DTIC-FDAC

1 MIAC/CINDAS, Purdue University, 2595 Yeager Road, West Lafayette,
   IN 47905

Commander, Army Research Office, P.O. Box 12211, Research Triangle Park,
NC 27709-2211
1 ATTN: Information Processing Office

Commander, U.S. Army Materiel Command, 5001 Eisenhower Avenue,
Alexandria, VA 22333
1 ATTN: AMCSCI

Commander, U.S. Army Materiel Systems Analysis Activity,
Aberdeen Proving Ground, MD 21005
1 ATTN: AMXSY-MP, H. Cohen

Commander, U.S. Army Missile Command, Redstone Scientific Information Center,
Redstone Arsenal, AL 35898-5241
1 ATTN: AMSMI-RD-CS-R/Doc
1   AMSMI-RLM

Commander, U.S. Army Armament, Munitions and Chemical Command, Dover, NJ 07801
1 ATTN: Technical Library

Commander, U.S. Army Natick Research, Development and Engineering Center,
Natick, MA 01760-5010
1 ATTN: Technical Library

Commander, U.S. Army Satellite Communications Agency, Fort Monmouth, NJ 07703
1 ATTN: Technical Document Center

Commander, U.S. Army Tank-Automotive Command, Warren, MI 48397-5000
1 ATTN: AMSTA-ZSK
1   AMSTA-TSL, Technical Library

Commander, White Sands Missile Range, NM 88002
1 ATTN: STEWS-WS-VT

President, Airborne, Electronics and Special Warfare Board, Fort Bragg,
NC 28307
1 ATTN: Library

Director, U.S. Army Ballistic Research Laboratory, Aberdeen Proving Ground,
MD 21005
1 ATTN: SLCBR-TSB-S (STINFO)

Commander, Dugway Proving Ground, Dugway, UT 84022
1 ATTN: Technical Library, Technical Information Division

Commander, Harry Diamond Laboratories, 2800 Powder Mill Road, Adelphi, MD 20783
1 ATTN: Technical Information Office

Director, Benet Weapons Laboratory, LCWSL, USA AMCCOM, Watervliet, NY 12189
1 ATTN: AMSMC-LCB-TL
1   AMSMC-LCB-R
1   AMSMC-LCB-RM
1   AMSMC-LCB-RP

Commander, U.S. Army Foreign Science and Technology Center, 220 7th Street, N.E.,
Charlottesville, VA 22901-5396
3 ATTN: AIFRTC, Applied Technologies Branch, Gerald Schlesinger

1 Plastics Technical Evaluation Center, (PLASTEC), ARDEC, Bldg. 355N,
   Picatinny Arsenal, NJ 07806-5000

Commander, U.S. Army Aeromedical Research Unit, P.O. Box 577, Fort Rucker,
AL 36360
1 ATTN: Technical Library

No. of Copies	To
	Commander, U.S. Army Aviation Systems Command, Aviation Research and Technology Activity, Aviation Applied Technology Directorate, Fort Eustis, VA 23604-5577
1	ATTN: SAVDL-E-MOS
	U.S. Army Aviation Training Library, Fort Rucker, AL 36360
1	ATTN: Building 5906-5907
	Commander, U.S. Army Agency for Aviation Safety, Fort Rucker, AL 36362
1	ATTN: Technical Library
	Commander, USACDC Air Defense Agency, Fort Bliss, TX 79916
1	ATTN: Technical Library
1	Clarke Engineer School Library, 3202 Nebraska Ave. North, Ft. Leonard Wood, MO 65473-5000
	Commander, U.S. Army Engineer Waterways Experiment Station, P. O. Box 631, Vicksburg, MS 39180
1	ATTN: Research Center Library
	Commandant, U.S. Army Quartermaster School, Fort Lee, VA 23801
1	ATTN: Quartermaster School Library
	Naval Research Laboratory, Washington, DC 20375
1	ATTN: Code 5830
1	Dr. G. R. Yoder - Code 6384
	Chief of Naval Research, Arlington, VA 22217
1	ATTN: Code 471
1	Edward J. Morrissey, WRDC/MLTE, Wright-Patterson Air Force, Base, OH 45433-6523
	Commander, U.S. Air Force Wright Research & Development Center, Wright-Patterson Air Force Base, OH 45433-6523
1	ATTN: WRDC/MLLP, M. Forney, Jr.
1	WRDC/MLBC, Mr. Stanley Schulman
	NASA - Marshall Space Flight Center, MSFC, AL 35812
1	ATTN: Mr. Paul Schuerer/EHO1
	U.S. Department of Commerce, National Institute of Standards and Technology, Gaithersburg, MD 20899
1	ATTN: Stephen M. Hsu, Chief, Ceramics Division, Institute for Materials Science and Engineering
1	Committee on Marine Structures, Marine Board, National Research Council, 2101 Constitution Ave., N.W., Washington, DC 20418
1	Librarian, Materials Sciences Corporation, 930 Harvest Drive, Suite 300, Blue Bell, PA 19422
1	The Charles Stark Draper Laboratory, 68 Albany Street, Cambridge, MA 02139
	Wyman-Gordon Company, Worcester, MA 01601
1	ATTN: Technical Library
	General Dynamics, Convair Aerospace Division, P.O. Box 748, Fort Worth, TX 76101
1	ATTN: Mfg. Engineering Technical Library
1	Department of the Army, Aerostructures Directorate, MS-266, U.S. Army Aviation R&T Activity - AVSCOM, Langley Research Center, Hampton, VA 23665-5225
1	NASA - Langley Research Center, Hampton, VA 23665-5225
1	U.S. Army Propulsion Directorate, NASA Lewis Research Center, 2100 Brookpark Road, Cleveland, OH 44135-3191
1	NASA - Lewis Research Center, 2100 Brookpark Road, Cleveland, OH 44135-3191
	Director, U.S. Army Materials Technology Laboratory, Watertown, MA 02172-0001
2	ATTN: SLCMT-TML
4	Authors

AD UNCLASSIFIED
UNLIMITED DISTRIBUTION

Key Words

VASE
XPS
RBS

U.S. Army Materials Technology Laboratory
Watertown, Massachusetts 02172-0001
CHARACTERIZATION OF OXIDE FORMED ON SILICON
BY EXPOSURE TO ATOMIC OXYGEN IN SPACE -
Louise C. Sengupta, Judith S. Brodkin,
Wolfgang Franzen, and Paul L. Segalyn

Technical Report MTL TR 92-1, February 1992, 18 pp-
illus-tables, D/A Project: A1205.AH84

The oxide formed on silicon by exposure to space on the long duration exposure facility (LDEF) has been examined using variable angle spectroscopic ellipsometry (VASE), Fourier transform infrared spectroscopy (FTIR), and X-ray photoelectron spectroscopy (XPS). The position of the silicon specimen on the satellite resulted in the formation of an oxide whose thickness varied with distance along the sample surface. Each transverse section of the surface was studied separately and compared to a region on the sample shielded from the oxygen flux in space by an aluminum bar. Film thickness and composition of the oxide were determined by a least square fit of the VASE data to a model surface using an effective medium approximation. The results revealed a nonporous oxide film with a thickness that increased from 350 Å to 1200 Å almost linearly along the sample. Furthermore, all of the experiments revealed an oxygen deficiency that increases with film thickness. Several other techniques were also performed on the sample to confirm these results. These results can be used to identify some of the oxide deposition parameters which occurred in the environment of the LDEF.